



Received: 2016.09.27
Accepted: 2016.10.18
Published: 2017.06.22

Authors' Contribution:

- A** Study Design
- B** Data Collection
- C** Statistical Analysis
- D** Data Interpretation
- E** Manuscript Preparation
- F** Literature Search
- G** Funds Collection

Computed Tomography (CT) and Magnetic Resonance (MR) Findings in Xanthogranulomatous Cholecystitis: Retrospective Analysis of Pathologically Proven 30 Cases – Tertiary Care Experience

Binit Sureka^{1ABCDDE}, Vaibhav Pratap Singh^{1BE}, S. Rajesh Rajesh^{1DE}, Shalini Laroia^{1AF}, Kalpana Bansal^{1AD}, Archana Rastogi^{2BD}, Chhagan Bihari^{2BD}, Ajeet Singh Bhadoria^{3BD}, Nikhil Agrawal^{4AF}, Asit Arora^{4AF}

¹ Department of Radiology/Interventional Radiology, Institute of Liver and Biliary Sciences, New Delhi, India

² Department of Pathology, Institute of Liver and Biliary Sciences, New Delhi, India

³ Department of Community Medicine, Institute of Liver and Biliary Sciences, New Delhi, India

⁴ Department of Hepato-Pancreato-Biliary (HPB) Surgery, Institute of Liver and Biliary Sciences, New Delhi, India

Author's address: Binit Sureka, Department of Radiology/Interventional Radiology, Institute of Liver and Biliary Sciences, D-1, Vasant Kunj, New Delhi-110070, India, e-mail: binitSUREKAPGJ@gmail.com

Summary

Background:

To study CT and MR findings in xanthogranulomatous cholecystitis (XGC).

Material/Methods:

Retrospective analysis of 30 histopathologically confirmed cases of XGC. Seventeen patients underwent CECT and 13 underwent MRI. The following features were studied – wall thickness, intramural nodules, pericholecystic stranding, wall thickness, THAD, fat in gallbladder wall, cholelithiasis, infiltration, biliary dilatation, lymph nodes, complications.

Results:

The majority of cases (22/30) showed discontinuous mucosal lining. Discontinuous mucosal lining was seen in all cases with wall thickness >10 mm, 75% of cases with wall thickness between 3–10 mm and none in normal wall thickness (p=0.03). Diffuse wall thickening was seen in 23 cases, focal thickening in 3 and polypoidal wall thickening in 2 cases. Polypoidal thickening was seen in gallbladder carcinoma. Intramural nodules were present in 87.5% of cases with discontinuous mucosal lining. Pericholecystic stranding was seen in 19, biliary dilatation in 12, liver infiltration in 13 and fat in 7 cases. Lymphadenopathy was seen in 1 case with gallbladder carcinoma. Four cases showed a signal drop in the intramural nodules on chemical shift MRI.

Conclusions:

Discontinuous mucosal lining is evident in xanthogranulomatous cholecystitis. Diffuse wall thickening, intramural nodules, continuous or discontinuous mucosal lining and cholelithiasis may indicate XGC rather than gallbladder carcinoma. Based on correlation with pathophysiological findings, we conclude that discontinuous mucosal lining is not an unusual finding in cases of XGC. Advances in knowledge: Being aware of the radiological findings described in this article may be helpful in making preoperative radiological diagnosis of XGC. Mucosal lining may be continuous or discontinuous in XGC.

MeSH Keywords:

Cholecystitis • Gallbladder Diseases • Gallbladder Neoplasms • Magnetic Resonance Imaging • Multidetector Computed Tomography

Abbreviations:

CT – computed tomography; CECT – contrast-enhanced computed tomography; MRI – magnetic resonance imaging; THAD/THID – transient hepatic attenuation/intensity difference; XGC – xanthogranulomatous cholecystitis

PDF file:

<http://www.polradiol.com/abstract/index/idArt/901728>

Background

Xanthogranulomatous cholecystitis (XGC) is an uncommon chronic fibro-inflammatory process involving the gallbladder. Pathologically, the disease is characterized by focal or diffuse inflammation and marked proliferative fibrosis along with macrophage and foamy cell infiltration [1].

The term was coined by McCoy in 1976 [2,3]. The incidence of XGC varies from 0.66% to 1.8% [4]. The epidemiological data in previous studies have shown that there is a higher incidence of XGC in the Indian population, with little variation in gender amongst regions [5]. Preoperative radiological diagnosis of this intriguing entity is challenging, as in the majority of cases it can be confused with gallbladder malignancy and other rare benign entities such as IgG4 cholecystitis, eosinophilic cholecystitis, gallbladder tuberculosis and actinomycosis of the gallbladder. Correct preoperative diagnosis of XGC is important as it has an impact on surgical planning and prognosis. In this retrospective study, we studied CT and MR features of 30 histopathologically confirmed cases of XGC.

Material and Methods

Patients

Approval for this retrospective study was obtained from the ethical board of the Institution.

The study included histopathologically proven cases of xanthogranulomatous cholecystitis. A total of 30 cases (19 males and 11 females; mean age 50.1 years, age range 15–83 years) were included in the study.

Examination protocol

Computed tomography (CT) examination protocol

Triphasic abdominal CT was performed on the GE Discovery 750HD Single-source Dual Energy CT scanner (Discovery CT 750HD; GE Healthcare, Milwaukee, WI). Non-ionic iodinated contrast material (100 ml, iodine concentration, 400 mg/ml) was injected through an 18 to 20-gauge antecubital intravenous cannula at the rate of 4 ml/s. Scans were acquired in the hepatic arterial, portal venous and hepatic venous phases using a Smart Prep Protocol with enhancement threshold set at 100 HU. The following examination parameters were used: detector coverage – 40 mm, table speed – 98.43 mm/s, rotation time – 0.6 s, pitch and speed of 0.984, section thickness – 1.5 mm, reconstruction interval – 5-mm, 100–120 kVp and 200–360 mA. Additional images were reconstructed with 0.625 mm reconstruction intervals for detailed interpretation.

MR imaging (MRI) protocol

MRI was performed in our department with a Signa HDxt 3.0-T scanner volume MR (GE, Fairfield, CT, USA). A body phased-array coil with eight elements, centered below the xiphoid process, was used for signal reception. We acquired coronal and axial T2-weighted (T2W), single-shot fast spin-echo (FSE) sequences, axial respiratory-triggered

fat-suppressed T2W FSE sequence and axial breath-hold T1-weighted (T1W) dual-echo spoiled gradient recalled-echo sequence. The following parameters were used for T1-weighted images: fast spoiled gradient-echo (FSPGR) dual echo sequence of TR=4.7 ms, TE (out-of-phase)=1.22 ms and TE (in-phase)=2.46 ms. The T1-weighted and T2-weighted images were obtained in the axial plane with FOV=35–40 cm and slice thickness=5–8 mm.

Image interpretation

The raw images were analyzed by three experienced radiologists; Radiologist 1 (B.S.) with 8.5 years of experience, Radiologist 2 (S.R.) with 8 years of experience and Radiologist 3 (V.P.S.) with 4 years of experience in interpreting CT and MR.

The following features were recorded: (1) Wall thickness – <3 mm/3–10 mm/>10 mm; (2) Intramural nodules: intramural nodules were defined as well-defined nodular areas within the gallbladder wall appearing hypodense on CT and hyperintense/hypointense on T2w/T1w images, respectively; (3) Pericholecystic fat stranding; (4) Pattern of wall thickness – focal/diffuse/polypoidal. Focal wall thickening was defined as involvement of <50% of the gallbladder wall. Diffuse gallbladder wall thickening was defined as involvement of >50% of the gallbladder wall. Polypoidal wall thickening was defined as focal polypoidal projections of the gallbladder wall; (5) Transient hepatic attenuation/intensity difference (THAD/THID) adjacent to the gallbladder fossa region: THAD/THID was defined as the difference in liver parenchymal enhancement adjacent to the gallbladder that was visible during the hepatic arterial phase; (7) Fat within the gallbladder wall. On CT, fat was depicted by attenuation of –20 to –120 HU. MR chemical shift imaging was used to depict intramural fat; (8) Mucosal lining – continuous/discontinuous; (9) Gallbladder calculi; (10) Infiltration into adjacent structures (liver, duodenum, hepatic flexure, anterior abdominal wall); (11) Biliary dilatation; (12) Locoregional lymph nodes; (13) Complications if any – abscess, gallbladder perforation and malignant transformation.

Results

Out of total 30 cases, 17 cases underwent CECT (contrast-enhanced computed tomography) and 13 cases underwent MRI (magnetic resonance imaging). Our institutional protocol consists of an ultrasound examination with MRI in clinically suspected cases of gallbladder pathology. CECT is performed when gallbladder malignancy is suspected. The age in our study varied from 15 to 83 years. Nineteen cases (63.3%) were male and 11 cases (36.6%) were female. The majority of cases had wall thickness in the range of 3 to 10 mm; it was seen in 24 cases (80%). Four cases had wall thickness larger than 10 mm. Two cases had normal wall thickness.

Discontinuous mucosal lining was seen in 22 cases (73.3%) and most of these cases had an associated intramural nodule/collection adjacent to the site of mucosal discontinuity (Figures 1–3). The remaining 8 cases had a continuous mucosal lining. Discontinuous mucosal lining was seen in



Figure 1. A 48-year-old female with xanthogranulomatous cholecystitis. Axial CECT image demonstrating multiple hypodense intramural nodules (arrows) with a mucosal defect and associated intramural and hepatic collection (asterisk).



Figure 2. Discontinuous mucosal lining in xanthogranulomatous cholecystitis. Axial T2-weighted MR image showing diffusely thickened gallbladder wall with discontinuous mucosal lining (arrow). Tiny T2-weighted hyperintense intramural nodules are also seen in the fundal region (arrowhead).

all cases of XGC with gallbladder wall thickness >10 mm, in 18 cases with wall thickness between 3–10 mm and in no cases with normal wall thickness (<3 mm); this was



Figure 3. Discontinuous mucosal lining and infiltration in XGC. Axial CECT image demonstrating diffuse thickening of gallbladder wall with irregular mucosal lining and loss of fat planes within the anterior abdominal wall (interrupted arrow) and the hepatic flexure of the colon (solid arrow).

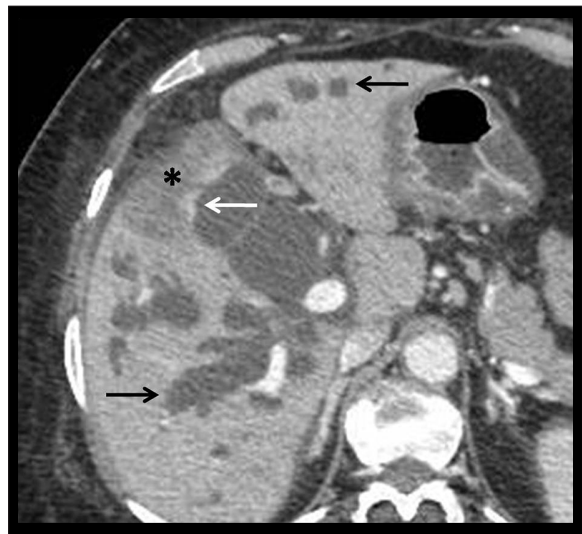


Figure 4. A 48-year-old female with concurrent xanthogranulomatous cholecystitis and carcinoma of gallbladder. Axial CECT image demonstrating polypoidal thickening in the fundal region (white arrow) associated with infiltration into the adjoining hepatic parenchyma (asterisk). Also seen is bilobar intrahepatic biliary dilatation (black arrows).

found to be statistically significant ($p=0.03$). The most common pattern of wall thickness was diffuse and it was seen in 23 cases (76.6%), whereas focal wall thickening was seen in only 3 cases (10%) and polypoidal thickening in 2 cases. The two cases of polypoidal thickening had overlapping features of XGC and gallbladder carcinoma on histopathology (Figure 4).

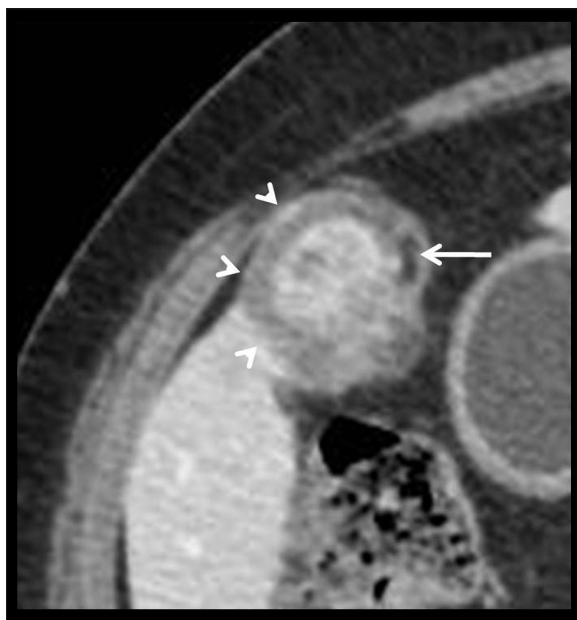


Figure 5. A 54-year-old female with xanthogranulomatous cholecystitis. Axial CECT image showing diffusely thickened gallbladder wall with hypodense intramural nodules (arrowheads) and intramural fat (arrow).

Intramural nodules were seen in a total of 16 cases (53.3%). Intramural fat was observed in 7 cases (Figure 5). Pericholecystic fat stranding was seen in 19 cases. Transient hepatic attenuation difference (THAD) adjacent to the gallbladder fossa region was seen in 8 cases. Intramural nodules were present in 14 cases with discontinuous mucosal lining and absent in 8 cases with discontinuous mucosal lining; however, this was not statistically significant ($p=0.06$). Pericholecystic fat stranding was seen in 19 (63.3%) cases.

Out of 13 patients who underwent MR imaging in our study, 12 cases had gallstones and 1 patient had biliary sludge. Biliary dilatation was seen in 12 cases (40%). Liver infiltration was seen in 13 cases. Eight cases had indistinct borders with the liver, while <2 cm of hepatic infiltration was seen in 4 cases, and only 1 case showed hepatic infiltration of more than 2 cm. Seventeen cases did not have hepatic infiltration. Apart from liver infiltration, other sites of pericholecystic infiltration were seen in our study, including duodenum in 5 cases. Three cases showed hepatic flexure infiltration. Anterior abdominal wall infiltration was seen in 2 cases. The liver was the most common site of pericholecystic infiltration in XGC. A significantly enlarged lymph node (>10 mm) was seen in only 1 case and this solitary case had a coexisting malignancy of the gallbladder. An associated liver abscess was seen in 4 cases. One patient had gallbladder perforation. The CT and MR findings are summarized in Table 1. The relationship between mucosal lining and the pattern of gallbladder wall thickness and intramural nodules is illustrated in Table 2.

On MR images, only 6 cases had visible intramural nodules. Among these 6 cases, the signal intensity of intramural nodule was higher on the in-phase image than on the out-of-phase image in 4 cases (Table 3).

Table 1. CT and MR findings in 30 patients with xanthogranulomatous cholecystitis.

CT and MR findings (CT – 17 patients; MR – 13 patients)	Number of patients (N=30)
Gallbladder wall thickness	
3–10 mm	24 (80%)
>10 mm	4 (13.3%)
<3 mm (normal wall thickness)	2 (6.6%)
Pattern of wall thickness	
Diffuse	23 (76.6%)
Focal	3 (10%)
Polypoidal	2 (6.6%)
Normal wall thickness	2 (6.6%)
Intramural hypodense/T2 hyperintense nodules	
Present	16 (53.3%)
Absent	14 (46.6%)
Intramural fat	
Absent	23 (76.6%)
Present	7 (23.3%)
Mucosal lining	
Discontinuous	22 (73.3%)
Continuous	8 (26.6%)
Pericholecystic fat stranding	
Present	19 (63.3%)
Absent	11 (36.6%)
Stones and dilatation	
Gallbladder stones	20 (66.6%)
Biliary dilatation	12 (40%)
Choledocholithiasis	5 (16.6%)
Infiltration of adjacent structures	
Infiltration into liver	13 (43.3%)
THAD/THID	8 (26.6%)
Infiltration into duodenum	5 (16.6%)
Infiltration into hepatic flexure	3 (10%)
Infiltration into abdominal wall	2 (6.6%)
Locoregional lymphadenopathy	
<10 mm	22 (73.3%)
>10 mm	1 (3.3%)
Complications	
Abscess	4 (13.3%)
Malignant transformation	3 (10%)
Pancreatitis	3 (10%)
Perforation	1 (3.3%)

THAD – transient hepatic attenuation difference; CT – computed tomography; MR – magnetic resonance imaging.

Discussion

Xanthogranulomatous cholecystitis was initially thought to be a malignant disease process, but now many studies have proven its benign course, similar to xanthogranulomatous pathologies involving other organs. The pathophysiology behind this intriguing disease involves mucosal trauma due to gallstones, production of lysolecithin and rupture of the Rokitansky-Aschoff sinuses, which results in spreading of

Table 2. Relationship between mucosal lining and pattern of gallbladder wall thickness and intramural nodules.

Mucosal lining	Wall thickness		Pattern of wall thickness		Intramural nodules	
	3–10 mm (n= 24)	>10 mm (n=4)	Diffuse (n=23)	Focal (n=3)	Present (n=16)	Absent (n=14)
Discontinuous (n=22)	18	4	18	3	14	8
Continuous (n=8)	6	0	5	0	2	6
<i>p</i> -Value*	<0.05		=0.05		=0.06	

* *p*-Value – Chi square statistics. The results suggest that diffuse gallbladder wall thickening, wall thickness >3 mm and intramural nodules in XGC are associated with a discontinuous mucosal lining.

Table 3. MR Signal intensity of intramural nodules and bile.

Cases	Signal Intensity of intramural nodules			Signal intensity of Bile		
	In-phase T1WI	Out-of-phase T1WI	Difference	In-phase T1WI	Out-of-phase T1WI	Difference
1	340	244	96	250	300	-50
2	750	531	219	680	500	180
3	350	406	-56	292	249	43
4	505	520	-15	270	300	-30
5	604	470	134	304	344	-40
6	665	568	97	270	240	30

Difference = (in-phase T1WI Signal intensity) – (out-of-phase T1WI Signal intensity).

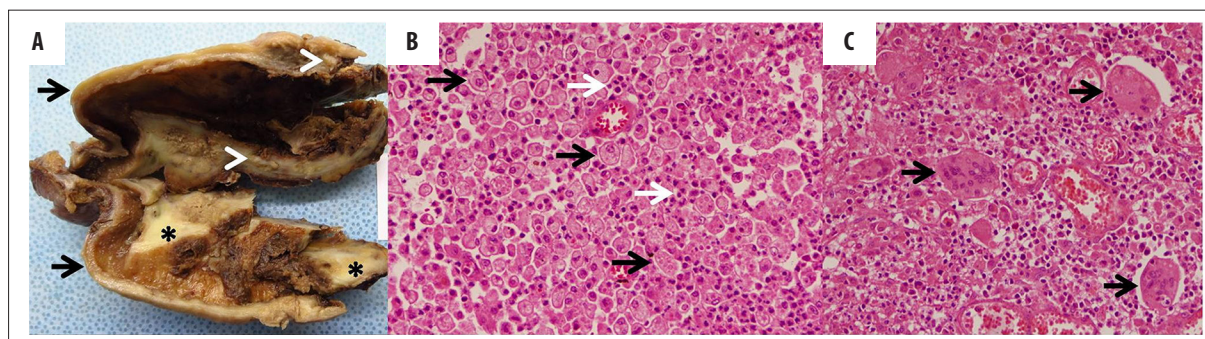


Figure 6. Histopathology of xanthogranulomatous cholecystitis. (A) Gross pathology specimen showing thickened wall of the gallbladder (arrows and asterisks) with xanthoma nodules (arrowheads). (B) High-power (200×) view showing sheets of histiocytes (black arrows) and lymphocytes (white arrow). (C) High-power (200×) view showing multinucleated giant cells (black arrows).

the inflammatory process to the adjacent tissues [6]. The degradation of bile results in phagocytosis of insoluble cholesterol and bile salts by histiocytes gives the characteristic XGC appearance of macrophage-laden and foamy histiocytes (Figure 6) [6].

Our study showed a male predilection, with a mean age of 50.1 years, which is similar to studies published previously [7]. The majority of cases (80%) had wall thickness between 3–10 mm, and the most common pattern of wall thickness was diffuse – seen in 23 cases. These results were similar to studies published in the literature [7,8].

Previous series have shown that continuous mucosal lining was more commonly seen in XGC, and gallbladder

carcinoma is more commonly associated with discontinuous mucosal lining [7–10]. However, in our experience, slightly different results were noted. The majority of subjects in our study (22 cases) showed discontinuous mucosal lining, and 8 cases showed continuous mucosal lining. Discontinuous mucosal lining was seen in 78.3% of cases with diffuse wall thickening and in 100% of cases with gallbladder wall thickness >10 mm. Intramural fat could be demonstrated in 7 cases (23.3%). Discontinuous mucosal lining was seen in 18.2% of cases with intramural fat. Intramural nodules were present in 87.5% of cases with discontinuous mucosal lining. A total of 20 (66.6%) cases in our study had gallstones. Biliary dilatation was seen in 12 cases. Out of these 12 cases, biliary dilatation was due to choledocholithiasis in 5 cases, due to coexisting gallbladder

carcinoma in 3 cases, due to pancreatitis-related biliary stricture in 3 cases and in 1 case the cause was not known.

In our series, a coexistence of the five features of diffuse thickened wall, wall thickness greater than 3 mm, presence of intramural hypodense nodule, discontinuous mucosal lining and gallbladder stones was seen in 8 subjects (26.7%), and 17 cases (56.7%) had a coexistence of at least four of these features. Our results are slightly different from what has been described in the literature [7–12]. The presence of discontinuous mucosal lining was more commonly seen in our series.

T1-weighted dual-echo chemical-shift MR with in-phase and out-of-phase imaging and apparent diffusion coefficient values have been used for the evaluation of XGC by some researchers [13,14]. The signal intensity of intramural nodules was higher on the in-phase image than on the out-of-phase image in 4 cases confirming fat/lipid within the wall.

The presence of discontinuous mucosal lining was more often seen in our case series in comparison to previously reported series. We put forward two reasons for the presence of discontinuous mucosal lining in XGC. One could be associated with a delayed presentation of patients, as our institution is a tertiary level referral center and probably

we are seeing a later phase of the disease. We are also unable to understand how could there be a continuous mucosal lining present in XGC when the pathophysiology itself is due to mucosal trauma and rupture of the sinuses of Rokitansky [6]. This question remains unanswered and is a gray zone for both the radiologist and pathologist with a potential for further research.

Conclusions

Coexistence of the five features, namely, diffusely thickened wall, wall thickness greater than 3 mm, presence of intramural hypodense nodules, continuous or discontinuous mucosal lining and gallbladder stones may suggest the possibility of xanthogranulomatous cholecystitis in a given clinical setting. Based on correlation with pathophysiological findings, we conclude that although discontinuous mucosal lining is more often seen in gallbladder carcinoma, it can also be seen in XGC, especially if associated with a combination of at least four of the above-mentioned features. In difficult and confusing cases, new and advanced MR techniques may be helpful.

Conflict of interest

The authors declare that they have no conflict of interest.

References:

- Rammohan A, Cherukuri SD, Sathyanesan J et al: Xanthogranulomatous cholecystitis masquerading as gallbladder cancer: Can it be diagnosed preoperatively? *Gastroenterol Res Pract*, 2014; 2014: 253645
- McCoy JJ Jr., Vila R, Petrossian G et al: Xanthogranulomatous cholecystitis. Report of two cases. *JSC Med Assoc*, 1976; 72: 78–79
- Christensen AH, Ishak KG: Benign tumors and pseudotumors of the gallbladder. Report of 180 cases. *Arch Pathol*, 1970; 90: 423–32
- Reed A, Ryan C, Schwartz S: Xanthogranulomatous cholecystitis. *J Am Col Surg*, 1994; 179: 249–52
- Hale MD, Roberts KJ, Hodson J et al: Xanthogranulomatous cholecystitis: A European and global perspective. *HPB (Oxford)*, 2014; 16: 448–58
- Sjodahl R, Tagesson C, Wetterfors J: On the pathogenesis of acute cholecystitis. *Surg Gynecol Obstet*, 1978; 146: 199–202
- Zhao F, Lu PX, Yan SX et al: CT and MR features of xanthogranulomatous cholecystitis: an analysis of consecutive 49 cases. *Eur J Radiol*, 2013; 82: 1391–97
- Chun KA, Ha HK, Yu ES et al: Xanthogranulomatous cholecystitis: CT features with emphasis on differentiation from gallbladder carcinoma. *Radiology*, 1997; 203: 93–97
- Goshima S, Chang S, Wang JH et al: Xanthogranulomatous cholecystitis: Diagnostic performance of CT to differentiate from gallbladder cancer. *Eur J Radiol*, 2010; 74: e79–83
- Chang BJ, Kim SH, Park HY et al: Distinguishing xanthogranulomatous cholecystitis from the wall-thickening type of early-stage gallbladder cancer. *Gut Liver*, 2010; 4: 518–23
- Singh VP, Rajesh S, Bihari C et al: Xanthogranulomatous cholecystitis: What every radiologist should know. *World J Radiol*, 2016; 8: 183–91
- Quatrino GM, Tan MC, Rostas JW et al: Xanthogranulomatous cholecystitis. *Am Surg*, 2015; 81: E349–50
- Hatakenaka M, Adachi T, Matsuyama A et al: Xanthogranulomatous cholecystitis: importance of chemical-shift gradient-echo MR imaging. *Eur Radiol*, 2003; 13: 2233–35
- Kang TW, Kim SH, Park HJ et al: Differentiating xanthogranulomatous cholecystitis from wall-thickening type of gallbladder cancer: Added value of diffusion-weighted MRI. *Clin Radiol*, 2013; 68: 992–1001